JOURNAL OF MATERIALS SCIENCE **38** (2003) 1623–1629

Thermoelectric properties of p- and n-type $FeSi_2$ prepared by spray drying, compaction and sintering technique

O. YAMASHITA, S. TOMIYOSHI
Faculty of Engineering, Ehime University, Bunkyocho, Matsuyama, 790-8577, Japan
E-mail: yamashio@eng.ehime-u.ac.jp

N. SADATOMI
Sumitomo Special Metals Company, Limited, 2-15-17, Egawa, Shimamoto-cho, Osaka, 618-0013, Japan

$FeSi_2$ alloys doped with Mn and Co (p-type $Fe_{0.926}Mn_{0.074}Si_2$, n-type $Fe_{0.980}Co_{0.020}Si_2$) were prepared by vacuum induction melting. The ingots were pulverized in a jet-mill, and the powders were granulated by spray drying method using aqueous polyvinyl alcohol (PVA) binder in order to investigate the possibility of production on a large scale. The powders granulated exhibited excellent characteristics of flowability, leading to the smooth feeding into a die cavity in compacting. The powders obtained were compacted at a pressure of 98 MPa. It was debindered at 723 K for 1 h and sintered at 1423 K for 5 h in a hydrogen atmosphere, so that the residual carbon and oxygen contents in a sintered body approached to those in the starting powder. Subsequently it was annealed at 1113 K for 100 h in an argon atmosphere, to produce the semiconducting β-$FeSi_2$ phase. The thermoelectric figures of merit (Z) for optimum p- and n-type $FeSi_2$ are 1.75×10^{-4} (K^{-1}) and 2.0×10^{-4} (K^{-1}) at about 900 K, respectively, which agree roughly with those obtained by Tani and Kido for $FeSi_2$ materials prepared by the spark plasma sintering method. It indicates that the spray drying method leading to the production on a large scale is available for the fabrication of the thermoelectric $FeSi_2$ materials.

1. Introduction

Semiconducting β-$FeSi_2$ is well known as an attractive material for high temperature thermoelectric conversion because of its large Seebeck coefficient, relatively low electrical resistivity, and high oxidation resistance [1, 2]. Many studies on the thermoelectric properties of β-$FeSi_2$ have hitherto been carried out to raise the thermoelectric figure of merit ($ZT = S^2T/\kappa\rho$), where S is the Seebeck coefficient, ρ is the electrical resistivity, κ is the thermal conductivity and T is the absolute temperature [2–11]. Therefore, a low lattice thermal conductivity and a low electrical resistivity are desirable for improvement of the figure of merit. The conduction types are p-type, produced by doping with vanadium, chromium, manganese and aluminum and n-type, produced by doping with cobalt, nickel, platinum and palladium [2–6, 8–14]. The most effective doping was obtained with manganese and aluminum for p-type β-$FeSi_2$, and with cobalt for n-type material [15]. In the present experiment, thus, the p- and n-type specimens were prepared by doping with manganese and cobalt, respectively, resulting in higher figures of merit (ZT) [11, 12].

According to the phase diagram of the Fe-Si system [16], the semiconducting β-$FeSi_2$ with an orthorhombic structure is stable below a phase transition temperature of 1255 K and peritectoidally decomposes into nonstoichiometric α-Fe_2Si_5 with a tetragonal structure and ε-FeSi with a cubic structure above 1255 K, both of which exhibit metallic conduction. As-solidified $FeSi_2$ has an eutectic structure which is composed of α- and ε-phases.

Both single-crystal and polycrystalline β-$FeSi_2$ materials are available for thermoelectric applications. The single-crystal β-$FeSi_2$ is obtained by annealing nonstoichiometric α-Fe_2Si_5 specimens prepared by the Czochralski or Bridgeman method, while the chemical vapor transport (CVT) reaction method [15, 17, 18] makes it possible to fabricate directly the single-crystal β-$FeSi_2$ without the annealing process. However, the single-crystal α-Fe_2Si_5 synthesized by Czochralski or Bridgeman method often breaks when the phase transition from α- to β-phase occurs [8]. In addition, as the single-crystal β-$FeSi_2$ is much too expensive, it would be hardly utilized as a thermoelement. Powder metallurgy method, therefore, is the only way to fabricate polycrystalline β-$FeSi_2$ on a large scale. As

conventional powder metallurgy methods, there are cold-pressing and sintering [9], hot-press (HP) [10] and spark plasma sintering (SPS) [11, 12] methods. None of their technologies, however, fits to the mass production, because their slow compacting and sintering cycles make products too expensive, although the main constituent elements are cheap materials.

Fine powders with poor flowability have been employed in the conventional powder metallurgy methods, to obtain a sintered body with higher density. When fine powders were used directly in the dry compaction, however, a common problem is variation in the quantity of powder fed into a die cavity from a powder feeder, which results in the variation in the dimensions of sintered bodies. In addition, the green body compacted using the raw powders without any binder was too brittle to handle, even when it was compacted at a high pressure. To avoid such a fracture, various types of organic binder have been utilized [3, 9].

Although $FeSi_2$ alloys are one of the promising materials for thermoelectric applications, the fabrication technologies on mass production have hitherto been hardly investigated. For this reason, as a fabricating process on a large scale, we examined the applicability of the spray drying process [19] to $FeSi_2$ powders, to improve both the flowability of powders and the mechanical strength of compacted bodies, because this process can not only provide firm green bodies, but also stabilize the dimensions of sintered products. Generally, fine powders are chemically aggressive and are apt to react with oxygen and carbon in organic binder. Such fine powders have made it more difficult to apply the spray drying process, because the thermoelectric properties of $FeSi_2$ alloy should be affected more or less by contamination of such impurities, which may result in some changes in the carrier concentration. As reported in our previous paper [20], however, we have already succeeded in applying this technique to the fabrication of Nd-Fe-B magnets [21] although their powders are more aggressive than the present powder, and demonstrated that it is possible to fabricate sintered bodies with excellent magnetic properties and high dimensional precision using spray drying method.

The purpose of this study is to investigate whether the spray drying method leading to the mass production is available for the fabrication of β-$FeSi_2$ alloys, and further whether the phase transition from metallic α- and ε-phases to a semiconducting β-phase occurs readily during annealing, even in spray dried and sintered $FeSi_2$ alloys.

2. Experiments

Two ingots of $Fe_{1-x}Mn_xSi_2$ ($x = 0.074$) and $Fe_{1-x}Co_xSi_2$ ($x = 0.020$) were prepared by vacuum induction melting method using iron (99.99% purity), silicon (>99.99% purity), manganese (99.9% purity) and cobalt (99.99% purity). The ingots were crushed by a stamp-mill and then pulverized using a jet-mill to obtain alloy powders with an average particle size of about 3–5 μm. The chemical analysis and average particle size of the powders used in the experiment are given in Table I. Fig. 1 shows the experimental procedures of spray drying.

When the spray drying technique is applied to the $FeSi_2$ alloy powders, it is necessary to investigate the degree to which the powders are oxidized and carbonized by an aqueous binder during the spray drying process. The $FeSi_2$ alloy powders are likely to react with both oxygen and carbon, which may result in the degradation of the thermoelectric characteristics. For this reason, the time dependence of the reaction of $FeSi_2$ powder with distilled water was investigated by analyzing the residual oxygen in powder placed in distilled water, held at 293, 303 and 333 K for various times.

The $FeSi_2$ powders were kneaded at 278 K in a polyvinyl alcohol (PVA) solution of concentration 10 wt%, in which the additive content of PVA itself was 0.5 wt%. Glycerin of 0.06 wt% as a plasticizer and distilled water were then added to the kneaded mixture to form a slurry with a solid content of 72 wt% and stirred for about 2 h in a stirring tank held at 278 K. The stirred slurry was supplied to the spray dryer apparatus from the slurry stirrer through rubber tubing and was sprayed out by the centrifugal force of the rotating disc, where the diameter of the rotary disc was 60 mm and rotational speed was 18000 rpm. The liquid droplets sprayed out into the drying chamber are instantaneously dried by a flow of heated nitrogen gas to form the granulated powder, where the inlet and outlet temperatures of the heated gas flow were set to 363 and 343 K, respectively. The oxygen concentration in the chamber was then maintained below 1%. The powder characteristics of granulated powders were measured using a powder tester such as Hall flow meter.

The granulated powders were compacted to a cylindrical shape of $\phi 15 \times 20$ mm^3 at a pressure of 98 MPa, using a die composed of cast iron. The debindering and sintering conditions were investigated in a hydrogen atmosphere and a vacuum, to decrease oxygen and carbon contents contained in compacted bodies. To obtain a sintered body with higher density, the green bodies debindered at 723 K were heated up to 1423 K at

TABLE I Results of chemical analysis and average particle size of Fe-Si alloy powders

Specimen		Composition						Average particle size (μm)
		Molecular unit (atomic ratio)				wt%		
No.	Type	Fe	Mn	Co	Si	O	C	
1	p	0.926	0.074	–	2	0.23	0.004	4.2
2	n	0.980	–	0.020	2	0.22	0.006	4.5

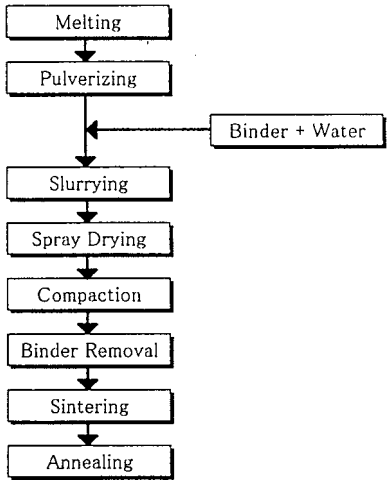

Figure 1 Experimental procedures of spray drying.

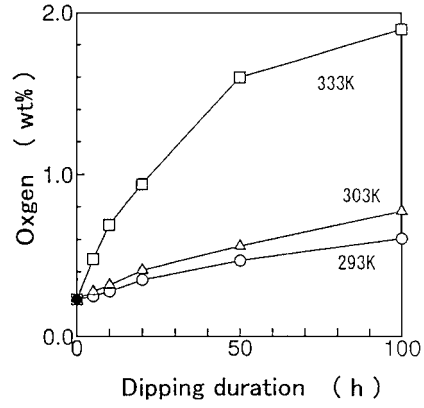

Figure 2 Relationship between duration of Fe-Si alloy powders dipped in distilled water and residual oxygen content.

heating rates of 75, 100 and 200 K/h and sintered at the maximum temperature for 5 h. This maximum temperature corresponds to one of the sintering temperatures employed by Cho *et al*. [9], when the green bodies compacted using $Fe_{0.9}Mn_{0.1}Si_2$ fine powders with 2–3 μm in diameter were sintered in an argon atmosphere.

The density of the sintered specimens was measured by the Archimedes method. The residual oxygen and carbon contents were determined using a Leco (Model IR-212) oxygen/carbon analyzer.

The sintered and annealed bodies were cut into parallelepipeds of $5 \times 5 \times 15$ mm^3 and square plates of $10 \times 10 \times 2$ mm^3. The former samples were subjected to Seebeck coefficient and electrical resistivity measurements (Sinku-Riko, Inc., Model ZEM-1), and the latter samples were ground into a disk of $\phi 10 \times 2$ mm^3 in order to measure the thermal conductivity using a laser-flash instrument (Sinku-Riko, Inc., Model TC-3000). The Seebeck coefficient S was measured with an accuracy of 5% by the conventional technique using Pt metal for electrodes in the temperature range from 323 to 1073 K with temperature difference of about 5 K. The electrical resistivity ρ was measured concurrently by the four-probe method. The thermal conductivity κ was measured at 298, 573 and 873 K.

The crystal structure of $FeSi_2$ before and after annealing was identified by X-ray diffraction analysis using Cu K_α radiation, and the microstructure of annealed specimens was investigated using an electron probe microanalyzer (EPMA) (JEOL, model JXA-8600MX).

3. Results and discussion

3.1. Spray conditions

As shown in Fig. 2, the residual oxygen content in powder placed in distilled water tends to increase gradually and linearly with time when the water temperature is 293 and 303 K, while at 333 K it increases abruptly with time. This indicates that the oxidation of $FeSi_2$ powder in water can be prevented as long as the water held below 293 K is used for only a short period of time when forming slurry.

In contrast, the residual carbon content resulting from binder addition was controlled by adding a smaller PVA binder content than that used in standard ceramic powders (1–2 wt%) and furthermore by removing the binder from the compacted body in a hydrogen atmosphere, as will be shown below. This small addition of PVA binder is particularly effective in reducing the residual oxygen and carbon contents [20].

The granulated powders prepared by using the $FeSi_2$ alloy powders (Nos. 1 and 2) were made almost spherical, as shown in Fig. 3. The average particle diameter of the granulated powders was about 70 μm in both powders (Nos. 1 and 2). The powder characteristics before and after spray drying are given in Table II. The flow rate was measured as the time required for 50 g of powder to fall gravitationally through a funnel tube with an orifice of 5 mm. Consequently, both loose and spatula angles of the raw powders before spray drying are too high to fall through an orifice at all, while the granulated powders (Nos. 1 and 2) showed lower loose and

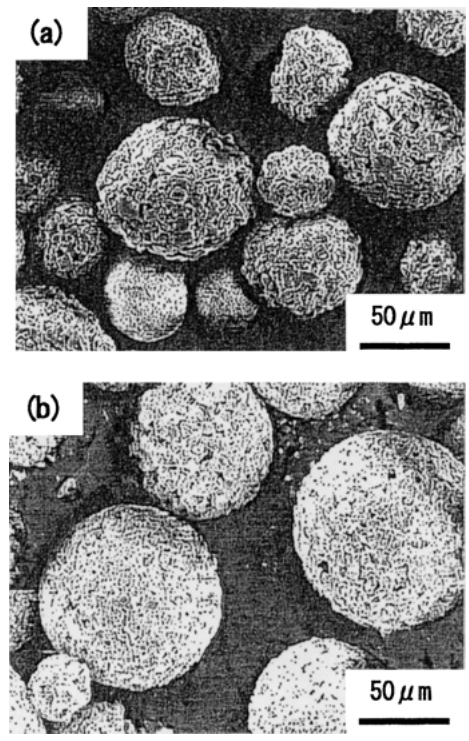

Figure 3 Scanning electron micrographs of p- (a) and n-type (b) $FeSi_2$ powders after spray drying.

TABLE II Powder characteristics of Fe-Si alloy powders before and after spray drying

Spray drying	Specimen no.	Average particle size (μm)	Apparent density (Mg/m^3)	Tap density (Mg/m^3)	Loose angle (deg)	Spatula angle (deg)	Flow rate[a] (sec/50 g · 5 ϕ)
As spray dried	1	72	1.27	1.38	28.2	36.5	9.07
As spray dried	2	71	1.34	1.46	27.1	37.2	8.87
As mixed	2	4.5	1.25	1.94	51.7	78.3	No flow
As spray dried	Ferrite	73	1.54	1.68	27.9	32.2	10.4

[a]Time required for 50 g of powder to fall gravitationally through a funnel tube with an orifice of 5 mm.

lower spatula angles, so that they fall naturally through an orifice at a short time. The present granulated powders exhibited almost the same flow rate as the powders granulated similarly by adding about 1 wt% PVA to an ordinary Mn-Zn ferrite powder, and it indicates that it is possible to feed smoothly the granulated $FeSi_2$ powders into a die cavity in dry compacting, because actually the granulated Mn-Zn powders have been fed smoothly in compacting. In addition, the relatively small difference between apparent density and tap density in the granulated powders indicates that the secondary particles are too hard to break into the primary particles.

3.2. Debindering and sintering

The residual oxygen and carbon contents after debindering at 723 K for 1 h and sintering at 1423 K for 5 h decreased markedly in a hydrogen atmosphere than in a vacuum, as listed in Table III, where the debindering temperature was determined in our previous work [20]. The oxygen and carbon contents after sintering in a hydrogen atmosphere decreased to about 60% and 10% of those contained in the granulated powders, respectively, but the oxygen and carbon contents in sintered bodies were about 0.1 and 0.02 wt% more than those in the raw powders, respectively.

As shown in Fig. 4, the relative bulk density depends strongly on the heating rate and tends to increase with increasing the heating rate. This is contrary to expectation. It is surprising that the relative density is very sensitive to the heating rate, particularly in a vacuum, although the reason is not clear. The relative density becomes higher in a hydrogen atmosphere than in a vacuum for any heating rate, and tends to saturate at a heating rate of 100 K/h in any atmosphere. The relative density obtained at a heating rate of 200 K/h in a hydrogen atmosphere was 98% for p-type $FeSi_2$ and 90% for n-type $FeSi_2$, in which the relative density of p-type specimen was higher than 95% obtained by Tani and Kido [11] for $Fe_{0.95}Mn_{0.05}Si_2$ prepared by SPS method, although the present specimen contains a large quantity (0.32 wt%) of oxygen, while that of n-type specimen was lower than 95% reported by Tani and Kido [12] for $Fe_{0.97}Co_{0.03}Si_2$ prepared by SPS method.

TABLE III Residual carbon and oxygen contents of Fe-Si alloy powder before and after sintering

Process	Specimen no.	Atmosphere during binder removing and sintering	Content (wt%) C	O
Before spray drying	2	–	0.006	0.22
After spray drying	2	–	0.34	0.51
After sintering	1	Hydrogen	0.03	0.32
	1	Vacuum	0.10	0.64
	2	Hydrogen	0.03	0.32
	2	Vacuum	0.10	0.62

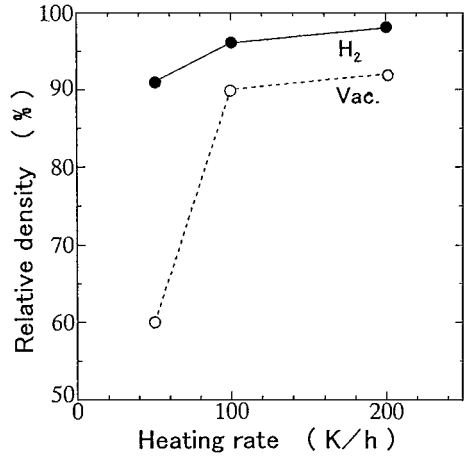

Figure 4 Relationship between heating rate and relative density of p-type $FeSi_2$, after sintering in a hydrogen atmosphere and a vacuum.

3.3. Annealing

In order to obtain the semiconducting phase (β-phase) of iron disilicide, the annealing conditions after sintering were investigated in the temperature range 1113–1233 K for 10–100 h under an argon atmosphere. Fig. 5 shows X-ray diffraction (XRD) patterns of p-type $FeSi_2$ annealed under various annealing conditions. The figure represents that major phases of an as-sintered specimen are α-Fe_2Si_5 and ε-FeSi, as expected from the phase diagram [16]. The intensity of peaks for α-Fe_2Si_5 tends to decrease abruptly with decreasing annealing temperature and disappears completely at 1113 K, while the peak intensity of peaks for ε-FeSi tends to decrease gradually with decreasing annealing temperature but remains even at a annealing temperature of 1113 K. When the annealing time at 1113 K was extended up to 100 h, the peak intensity of the β-$FeSi_2$ increased and that of the ε-FeSi decreased. These phase transitions are explained by the experimental results [22, 23] that there exist transition temperatures in the peritectoid reaction; "high temperature transformation temperature (1268 K)" below which α-$Fe_2Si_5 + \varepsilon$-FeSi $\rightarrow$ β-$FeSi_2$ takes place and "low temperature transformation temperature (1138 K)" below which primary transformation of "α-$Fe_2Si_5 \rightarrow \beta$-$FeSi_2 + Si$" and secondary transformation of "$Si + \varepsilon$-FeSi $\rightarrow \beta$-$FeSi_2$" take place in iron silicides. The phase transition of n-type

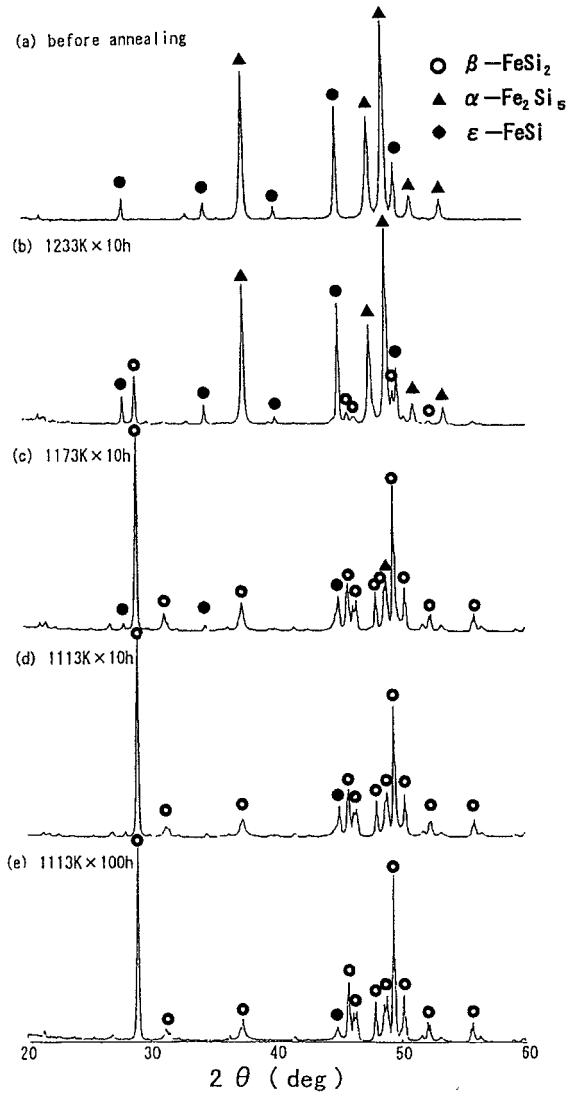

Figure 5 X ray diffraction patterns of p-type $FeSi_2$ annealed under various annealing conditions.

specimen also showed a tendency similar to that of p-type specimen, but the very weak peaks of residual α-Fe_2Si_5 phase were detected in an n-type specimen, in addition to the peaks of ε-FeSi phase.

Fig. 6 shows micrographs (above) and EPMA analyses (below) of p- and n-type $FeSi_2$ specimens prepared by the optimum fabricating conditions, which were sintered at 1423 K for 5 h in a hydrogen atmosphere and then annealed at 1113 K for 100 h in an argon atmosphere. In the micrographs both the small dark spots seen in p-type specimen (a) and the relatively larger dark spots or regions present in n-type specimen (b) represent pores, and these results are consistent with the magnitudes of relative densities of their specimens. Quantitative analysis of Si contents of each phase was made by EPMA, so that it was turned out that the broad dark regions and the numerous grey spots seen in both p- (c) and n-type (d) specimens are β- and ε-phases, respectively, and the small white spots present in an n-type specimen (d) alone are α-phases. These results of EPMA were entirely consistent with those of XRD. It was thus found that an ordinary phase transition occurs in the specimens prepared by spray drying.

3.4. Thermoelectric properties

Fig. 7a and b show the temperature dependence of Seebeck coefficients S and electrical resistivity ρ for p- and n-type $FeSi_2$ specimens prepared by the optimum fabricating conditions described above.

The p-type specimen has a large S of 450 μV/K at 323 K and tends to decrease slowly with temperature. The S at 323 K and its temperature dependence agree with those obtained by Tani and Kido [11] for $Fe_{0.95}Mn_{0.05}Si_2$ prepared by SPS method, although the ρ at 323 K of the present specimen is about 23% lower than 1.18×10^{-4} Ωm of $Fe_{0.95}Mn_{0.05}Si_2$. This

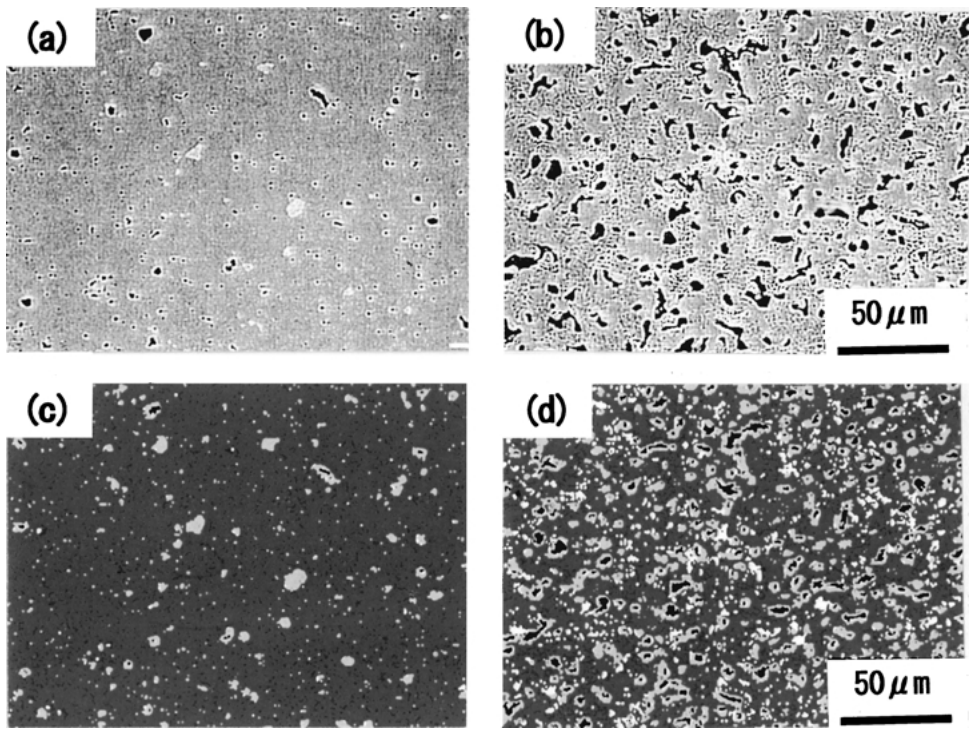

Figure 6 Scanning electron micrographs (above) and EPMA (below) analysis of p- ((a) and (c)) and n-type ((b) and (d)) $FeSi_2$ after annealing.

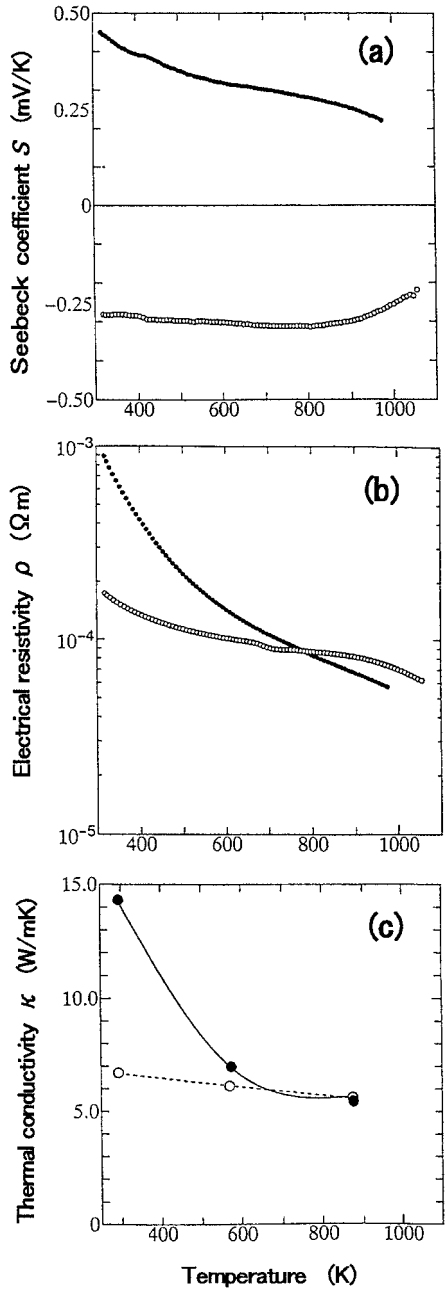

Figure 7 Temperature dependence of Seebeck coefficient S (a), electrical resistivity ρ (b) and thermal conductivity κ (c) for p- (●) and n-type (○) $FeSi_2$.

discrepancy would result from the difference in the relative density, because the relative density of the present specimen is about 3% high as compared with 95% of $Fe_{0.95}Mn_{0.05}Si_2$, as described above. Therefore, the agreement of these S values may indicate that the ρ values of the crystal grains themselves present in both polycrystalline specimens are almost the same. However, the present S at 323 K is 47% higher than 310 μV/K obtained by Kojima [3] for hot-pressed $Fe_{0.94}Mn_{0.06}Si_2$, which reflects the result that the ρ at 323 K is about 40% higher than 6.42×10^{-4} Ωm of $Fe_{0.94}Mn_{0.06}Si_2$.

In contrast, the absolute S of n-type specimen increases slightly with temperature, reaches a broad maximum at 800 K and then falls slowly above that temperature. The S at 323 K and its temperature dependence of n-type specimen agree closely with that obtained by Tani and Kido [12] for $Fe_{0.97}Co_{0.03}Si_2$ prepared by SPS method. This is entirely consistent with the fact that the ρ of n-type specimen coincides well with that of $Fe_{0.97}Co_{0.03}Si_2$; the ρ at 323 K is 1.74×10^{-4} Ωm for the present specimen and 1.67×10^{-4} Ωm for $Fe_{0.97}Co_{0.03}Si_2$ [12]. It is strange that although the Co content and the relative density of n-type specimen are less and lower than those of $Fe_{0.97}Co_{0.03}Si_2$, they have almost the same ρ value. This would be interpreted as follows; the rate of decrease in ρ due to the presence of two metallic ε-FeSi and α-Fe_2Si_5 phases present slightly in n-type specimen overcame the rate of increase in ρ due to the decrease in the relative density, so that the ρ of n-type specimen approaches that of $Fe_{0.97}Co_{0.03}Si_2$.

Fig. 7c shows the temperature dependence of thermal conductivity κ for p-type $Fe_{0.926}Mn_{0.074}Si_2$ and n-type $Fe_{0.98}Co_{0.02}$. The κ of n-type specimen decreases slowly and linearly with temperature, while the κ of p-type specimen decreases more rapidly with increasing temperature and approaches almost that of n-type specimen at about 700 K. Generally, the κ is the sum of the contributions arising from the lattice (κ_{ph}) and the electronic (κ_{el}) components. In order to understand the thermal conductivity behavior, the κ_{el} values of the present specimens were calculated using the Wiedemann-Franz law [24], $\kappa_{el} = L\sigma T$, where L is Lorentz number 2.45×10^{-8} V^2/K^2, σ is the electrical conductivity and T is the absolute temperature. As a result, the ratios of κ_{el} to κ_{ph} for both specimens are less than 1% at 300 K and are 4–6% at 873 K. Therefore, the thermal conductivities of the present specimens are mainly influenced by κ_{ph}. Generally, the increase in the dopant content tends to enhance the phonon scattering due to lattice short-range distortions, resulting in the decrease in κ_{ph}. However, the κ at 298 K of p-type specimen was about 15% larger than 12.4 W/mK at 300 K of $Fe_{0.95}Mn_{0.05}Si_2$, although the Mn content of the present specimen is about 1.5 times more than that of $Fe_{0.95}Mn_{0.05}Si_2$ [11]. Probably, such a discrepancy may result from the difference in the relative density; the higher the relative density, the larger the κ value, and indeed the relative density of the present specimen is 3% higher than 95% of $Fe_{0.95}Mn_{0.05}Si_2$ [11]. On the other hand, the κ at 298 K of n-type specimen was almost the same as 6.34 W/mK at 300 K of $Fe_{0.97}Co_{0.03}Si_2$ [12], although the Co content in the n-type specimen is 2/3 times of that in $Fe_{0.97}Co_{0.03}Si_2$. This would be attributed to a low relative density of n-type specimen, which is 5% low as compared with 90% of $Fe_{0.97}Co_{0.03}Si_2$. Over the wide temperature range from 298 to 873 K, however, the temperature dependences of κ for p- and n-type specimens exhibited a tendency similar to those of $Fe_{0.95}Mn_{0.05}Si_2$ [11] and $Fe_{0.97}Co_{0.03}Si_2$ [12] prepared by SPS method.

Subsequently, the Z values for p-type $Fe_{0.926}Mn_{0.074}Si_2$ and n-type $Fe_{0.98}Co_{0.02}$ were calculated from the relation $Z = S^2/\kappa\rho$ using the experimental values, where the κ values at temperatures except 298, 573 and 873 K were estimated by interpolating or extrapolating with a smooth curve

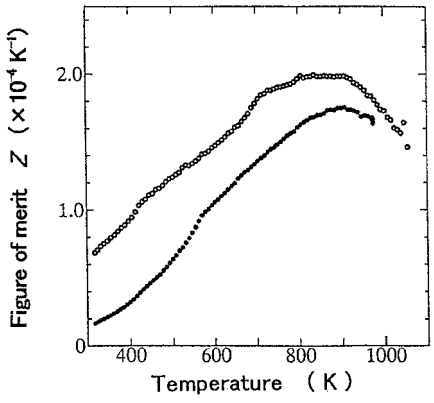

Figure 8 Temperature dependence of thermoelectric figure of merit Z for p- (●) and n-type (○) $FeSi_2$.

fitted well to the experimental data, as shown in Fig. 7c. As shown in Fig. 8, the resultant Z values for p-type $Fe_{0.926}Mn_{0.074}Si_2$ and n-type $Fe_{0.98}Co_{0.02}$ increase linearly with temperature, reach a maximum at about 900 K and fall rapidly with temperature. The maximum $Z$for p-type $Fe_{0.926}Mn_{0.074}Si_2$ is 1.75×10^{-4} (K^{-1}), which just corresponds to an intermediate value between two maximum Zvalues of 1.5×10^{-4} (K^{-1}) for $Fe_{0.95}Mn_{0.05}Si_2$ [11] and 1.9×10^{-4} (K^{-1}) for $Fe_{0.90}Mn_{0.10}Si_2$ [11]. On the other hand, the maximum Z for n-type $Fe_{0.98}Co_{0.02}Si$ is 2.00×10^{-4} (K^{-1}), which lies between two maximum Z values of 1.2×10^{-4} (K^{-1}) for $Fe_{0.99}Co_{0.01}Si_2$ [12] and 2.1×10^{-4} (K^{-1}) for $Fe_{0.97}Co_{0.03}Si_2$ [12]. It indicates that the $FeSi_2$ materials fabricated by spray drying method have almost the same thermoelectric properties as those prepared by SPS method. From these results, the spray drying method leading to the mass production, thus, was found to be available for the fabrication of β-$FeSi_2$ alloys with excellent thermoelectric properties.

4. Summary

The present experimental results can be summarized as follows.

(1) The p- and n-type $FeSi_2$ materials doped with 7.4 at.% Mn and 2.0 at.% Co, respectively, were melted by vacuum induction. After the ingots had been pulverized using a jet-mill, the fine powders were granulated by a spray dryer. The green bodies compacted using granulated powders were debindered and sintered in a hydrogen atmosphere and then annealed in an argon hydrogen atmosphere. The Co- and Mn-doped $FeSi_2$ materials prepared by such a fabricating process have almost the same thermoelectric properties as those reported previously by Tani and Kido [11, 12] for doped $FeSi_2$ materials prepared by SPS method on a laboratory scale.

(2) It was turned out that the residual oxygen and carbon contents in the sintered $FeSi_2$ can be reduced significantly by adding a content of 0.5 wt% PVA as a binder to the raw powder, stirring in a tank held at a temperature of 278 K, and debindering and sintering in a hydrogen atmosphere after compacting. In addition, the heating rate in the temperature range from debindering to sintering temperature was very important to obtain a sintered $FeSi_2$ with high density, and the higher density was found to be obtained when the heating rate is higher than 100 K/h.

(3) As the spray dried $FeSi_2$ powder fits well to the rapid compaction cycle owing to its high flowability, it was found to be very suitable for the mass production at low cost. Moreover, such an excellent flowability would help to produce a compacted body with homogeneous density in any place of a compacted green body, which results in the stabilization of both thermoelectric characteristics and dimensions in thermoelectric materials.

Acknowledgements

The authors wish to thank T. Saigo and M. Noumi of Sumitomo Special Metals Company for valuable technical support.

References

1. D. M. ROWE, "CRC Handbook of Thermoelectrics" (CRC Press, NewYork, 1995) p. 287.
2. I. NISHIDA, *Phys. Rev.* B **7** (1973) 2710.
3. T. KOJIMA, *Phys. Status Solidi* A **111** (1989) 233.
4. U. BIRKHOLZ and J. SCHELM, *ibid.* **27** (1968) 413.
5. J. HESSE and K. BUCKSON, *J. Mater. Sci.* **5** (1972) 272.
6. I. NISHIDA, *ibid.* **7** (1972) 1119.
7. T. SAKATA, Y. SAKAI, H. YOSHINO and H. FUJII, *J. Less-Comm. Metals* **61** (1978) 301.
8. E. GROß, M. RIFFEL and U. STÖHRER, *J. Mater. Res.* **10** (1995) 34.
9. W. S. CHO, S. W. CHOI and K. PARK, *Mater. Sci. Eng.* B **68** (1999) 116.
10. H. TAKIZAWA, P. F. MO, T. ENDO and M. SHIMADA, *J. Mater. Sci.* **30** (1995) 4199.
11. J. TANI and H. KIDO, *J. Ceram. Soc. Japan* **109** (2001) 557.
12. *Idem.*, *Jpn. J. Appl. Phys.* **40** (2001) 3236.
13. *Idem.*, *J. Appl. Phys.* **84** (1998) 1408.
14. *Idem.*, *ibid.* **88** (2000) 5810.
15. A. HEINRICH, H. GRIESSMANN, G. BEHR, K. IVANENKO, J. SCHUMANN and H. VINZELBERG, *Thin Solid Films* **381** (2001) 287.
16. R. HULTGREN, P. D. DESAI, D. T. HAWKINS, M. GLEISER and K. K. KELLEY, "Selected Values of Binary Alloy" (*Am. Soc. for Metals*, Ohio, 1973) p. 873.
17. G. BEHR, J. WERNER, G. WEISE, A. HEINRICH, A. BURKOV and C. GLADUN, *Phys. Status Solidi* A **160** (1997) 549.
18. C. H. KLOC, E. ARUSHANOV, M. WENDL, H. HOHL, U. MALANG and E. BUCHER, *J. Less-Comm. Metals* **219** (1995) 93.
19. K. MASTER, "Spray Drying Handbook" (Longman Scientific & Technical, Harlow, 1991) p. 23.
20. O. YAMASHITA and Y. KISHIMOTO, *Powder Metall.* **41** (1998) 177.
21. M. SAGAWA, S. FUJIMURA, N. TOGAWA, H. YAMAMOTO and Y. MATSUURA, *J. Appl. Phys.* **55** (1984) 2083.
22. T. KOJIMA, M. OKAMOTO and I. NISHIDA, in Proceedings of the 5th International Conference on Thermoelectric Energy Conversion, Arlington, March, 1984, p. 56.
23. S.-C. UR, I.-H. KIM and J.-L. LEE, *Metals and Materials International* **8** (2002) 169.
24. See, for example, "Semiconductor Physics" (Springer, Seeger, Berlin, 1997) p. 77.

Received 16 July
and accepted 11 December 2002